Rare Metal Materials and Engineering
Volume 50, Issue 11, November 2021
Available online at www.rmme.ac.cn

Science Press

Cite this article as: He Haoran, Liu Qi, Bo Xinwei, et al. In-situ Fabrication of (Ti, Mo)Si_2/$MoSi_2$ Composite Coating to Protect Mo Substrate Against Cyclic Oxidation at 1200 ° C[J]. Rare Metal Materials and Engineering, 2021, 50(11): 3828-3836.

ARTICLE

In-situ Fabrication of (Ti, Mo)Si_2/$MoSi_2$ Composite Coating to Protect Mo Substrate Against Cyclic Oxidation at 1200 °C

He Haoran[1,3], **Liu Qi**[1,2,3], **Bo Xinwei**[1,2], **Wang Xiaoyu**[1], **Wang Yanhui**[1], **Yao Zhiyuan**[1], **Han Xiaoyu**[1], **Liu Chengchao**[1]

[1] Chongqing Materials Research Institute Co., Ltd, Chongqing 400707, China; [2] National Engineering Research Center for Instrument Function Materials, Chongqing 400707, China; [3] School of Chemistry and Chemical Engineering, Chongqing University of Technology, Chongqing 400054, China

Abstract: (Ti, Mo)Si_2/$MoSi_2$ composite coatings were prepared on Mo substrate by the continuous deposition pack cementation method. The X-ray diffraction (XRD), scanning electron microscope (SEM), energy dispersive spectroscopy (EDS), and thermodynamic calculation were used to characterize the composite coatings and to analyze the formation mechanism. The results show that the co-deposition process cannot achieve the titanium deposition effectively. The titanium-modified $MoSi_2$ coatings can be prepared by a two-step deposition process of titanizing and siliconizing. The coatings contain three layers: the outer layer is (Ti, Mo)Si_2 ternary compound layer; the second layer is $MoSi_2$ layer; the layer between the $MoSi_2$ and Mo substrate is the Mo_5Si_3 transition layer. The siliconizing temperature shows negligible effect on coating structure. The growth rate of titanium-modified $MoSi_2$ coating is slightly lower than that of single $MoSi_2$ coating. The growth of (Ti, Mo)Si_2/$MoSi_2$ composite coating is dominated by the inward diffusion of Ti and Si. Ti is concentrated on the outer layer of the coating. Si diffuses through the (Ti, Mo)Si_2 compound layer and interacts with the substrate to form the $MoSi_2$ layer and Mo_5Si_3 transition layer. In the titanizing process, the free state AlF_3 is introduced by the reaction among pack mixtures. In the subsequent siliconizing process, a trace amount of Al in free state is precipitated in the form of Al_3Mo phases in the (Ti, Mo)Si_2 layer near the upper interface of $MoSi_2$ layer. During the cyclic oxidation tests at 1200 °C, the (Ti, Mo)Si_2/$MoSi_2$ composite coatings do not lose mass obviously after exposure in oxidation atmosphere for 180 h. A dense composite oxide layer consisting of SiO_2 and TiO_2 can be formed by the oxidation of (Ti, Mo)Si_2 phase. This composite oxide layer can fill the surface cracks of the coating and continuously block the oxygen diffusion, so the oxidation resistance of (Ti, Mo)Si_2/$MoSi_2$ composite coating in the periodic oxidation environment is far superior to that of the single $MoSi_2$ coating.

Key words: pack cementation; molybdenum disilicide; titanium modification; anti-oxidation

Molybdenum has been widely used in electronic devices, heater elements, glass fiber processing, thermometry protective tubes, and aero-space crafts due to its excellent high-temperature properties. However, the poor antioxidation ability restricts the further application of molybdenum under high temperature atmosphere[1-3]. The silicide coating prepared on Mo substrate has been extensively researched, because $MoSi_2$ can form the dense SiO_2 layer on the coating surface, which can hinder the oxygen diffusion into the matrix and fill the cracks, holes, and other defects caused by thermal expansion during the high temperature oxidation[4-6]. However, the strength and creep resistance of the $MoSi_2$ coating at high temperature is poor, and it is easy to cause the spalling of SiO_2 under thermal cycle process, which reduces the anti-oxidation life of the coating[7,8]. The oxidation resistance of $MoSi_2$ can be effectively improved and the pesting oxidation can be inhibited by adding other elements into $MoSi_2$, especially the ones with greater affinity to oxygen than to Si. The addition of alloying elements can form the protective oxide film during the oxidation process[9,10]. Yanagihara et al[8] showed that adding Ti in $MoSi_2$ can produce selective oxidation at $MoSi_2$ grain boundary, thus inhibiting the pesting effect. Boettinger

---

Received date: November 07, 2020
Foundation item: Sponsored by Basic Research and Frontier Exploration of Chongqing (cstc2019jcyj-msxmX0795); Major Science and Technology Projects of Nuclear Power (2017ZX06004004); Technology Innovation and Application Demonstration Project of Beibei (2020-4)
Corresponding author: Liu Qi, Master, Senior Engineer, Chongqing Materials Research Institute Co., Ltd, Chongqing 400707, P. R. China, Tel: 0086-23-60315485, E-mail: liuqi@cmri.cc

et al[11] reported that titanizing of $MoSi_2$ can form the (Ti, Mo)Si_2 phase with C40 structure, and the duplex phase structure composed of C11b $MoSi_2$ and C40 (Ti, Mo)Si_2 performs good thermal stability and ductility at high temperatures[12]. Li et al[13] prepared (Ti, Mo)Si_2/$MoSi_2$ composite coating by slurry sintering method. The (Ti, Mo)Si_2 is dispersed in $MoSi_2$, and this coating can be oxidized at 1500 °C for 40 h without mass loss. Thus, the synthesis of (Ti, Mo)Si_2/$MoSi_2$ coating on the Mo surface can improve the oxidation resistance.

The methods used to prepare element-modified $MoSi_2$ coating include pack cementation, chemical vapor deposition, thermal spraying, slurry, etc[14-17]. Compared with other methods, the pack cementation method has been widely used for its advantages of simple process, low cost, no restriction of specimen shape, and high bonding strength between the coating and the matrix[18]. However, the preparation of titanium-modified $MoSi_2$ coating by pack cementation has rarely been reported. Therefore, the titanium-modified $MoSi_2$ coatings by pack cementation method were prepared in this research. The influence of different pack cementation methods on coating structure was investigated and the effective synthetic route was developed. The influence of siliconizing temperature and siliconizing time after titanizing of the (Ti, Mo)Si_2/$MoSi_2$ composite coatings was investigated, and the formation mechanism of (Ti, Mo)Si_2/$MoSi_2$ composite coatings formed by deposition of Ti and Si was studied. Finally, the cyclical oxidation resistance of the composite coatings at 1200 °C was also evaluated.

1 Experiment

The molybdenum rods (hot working state, purity of 99.5%) were used as the substrates for coating experiment. Cylindrical specimens with the dimension of Φ12 mm×6 mm were obtained by electric-discharge machining. After polishing by 800# SiC paper, the specimens were cleaned ultrasonically in ethanol and then dried. Two kinds of pack cementation methods were employed to prepare (Ti, Mo)Si_2/$MoSi_2$ composite coatings. (1) Co-deposition method: prepare the coatings at 1000 °C for 5 h in Ar atmosphere with the pack mixture containing different contents of Ti and Si. The final product prepared by co-deposition method is named as xTi-ySi-10NH_4F-50Al_2O_3. (2) Two-step deposition method (titanizing-siliconizing): firstly prepare the Ti-modified layer at 1000 °C for 5 h in Ar atmosphere with the pack mixture and obtain the intermediate product of 40Ti-10NH_4F-50Al_2O_3 (wt%); then process the intermediate product at 900~1100 °C for 1~9 h. The specimens with single $MoSi_2$ layer were also prepared at 1000 °C for 1~9 h as the control group. The effect of deposition kinetic parameters of coating preparation on oxidation resistance of coatings was investigated, as shown in Table 1.

The pack mixtures consisted of NH_4F (activator), Al_2O_3 (filler), and Si/Ti (Si source/Ti source), which were mixed in a ball mill for 2 h. The specimens were embedded in cylindrical alumina crucibles sealed with alumina lids using silica sol binder. The sealed crucibles were then inserted into a horizontal tube furnace with a flowing Ar atmosphere (purity of 99.999%, 30 mL/min). After the Ar atmosphere was established, the furnace was heated up to the setting temperature for coating preparation.

Periodic oxidation tests were conducted in a horizontal tube furnace from room temperature to 1200 °C. The (Ti, Mo)Si_2/$MoSi_2$ composite coatings prepared by the two-step pack cementation method and the single $MoSi_2$ coating were separately placed in the alumina crucibles of high-purity and then the alumina crucibles were put into the horizontal tubular furnace. The furnace was heated from room temperature to 1200 °C at a heating rate of 20 °C/min in the atmosphere for 10 h, and then the crucibles were taken out for air-cooling to room temperature, which was recorded as an oxidation cycle. After each oxidation cycle, the mass change of specimens was measured by an electronic balance (balance precision of 0.1 mg). The mass changes of the specimens with increasing the oxidation time were also recorded.

Scanning electron microscopy (SEM, TESCAN VEGA3) was used to observe the surface and cross section morphologies of the coatings. The chemical composition of the coatings was analyzed by energy dispersive spectroscopy (EDS, TESCAN VEGA3). X-ray diffraction (XRD, X'pertpro MPD) was used to analyze the phases of coatings and pack mixtures after pack cementation.

2 Results and Discussion

2.1 Phase composition and microstructure of coatings

Fig. 1 shows the coating phase component, the backscattered

Table 1 Process parameters of coating preparation

Method		Temperature/°C	Time/h	Composition of pack mixture/wt%			
				Ti	Si	NH_4F	Al_2O_3
Co-deposition cementation		1000	5	20	20	10	50
				15	25		
				10	30		
Two-step pack cementation	Titanizing	1000	5	40	-	10	50
	Siliconizing	900	5	-	40		
		1000	1, 3, 5, 7, 9	-	40		
		1100	5	-	40		
Single-layer cementation		1000	1, 3, 5, 7, 9	-	40	10	50

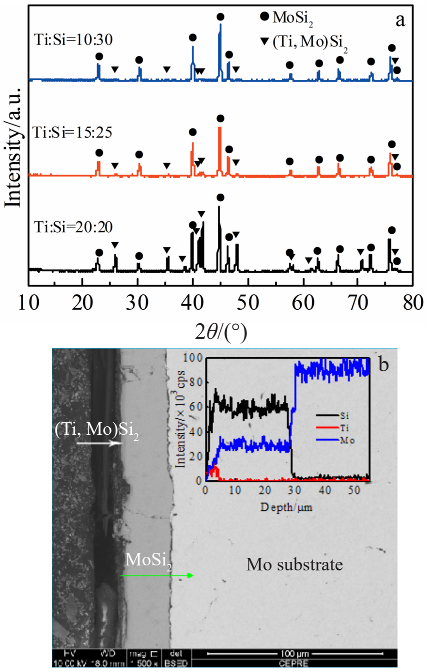

Fig.1 XRD patterns of coatings prepared by co-deposition (a); BSE image and EDS element line scanning result of 20Ti-20Si-10NH$_4$F-50Al$_2$O$_3$ coating (b)

electron (BSE) image of the cross section of coatings, and EDS element line scanning result of the coating prepared by co-deposition method at 1000 °C for 5 h. The diffraction peaks in Fig. 1a correspond to the (Ti, Mo)Si$_2$ and MoSi$_2$ phases, which indicates that the addition of Ti modifies the phases of coatings. The coatings display a two-phase structure with C40 (Ti, Mo)Si$_2$ and C11b MoSi$_2$[19]. Meanwhile, with decreasing the Ti content in pack mixtures, the diffraction peaks of (Ti, Mo)Si$_2$ phase are weakened, suggesting that the content of (Ti, Mo)Si$_2$ phase is also decreased. Fig. 1b shows the BSE image and elemental line distribution of the cross section of 20Ti-20Si-10NH$_4$F-50Al$_2$O$_3$ coating. The discontinuous (Ti, Mo)Si$_2$ layer with a thickness of 3~5 μm in the outer layer can be observed, and the second layer is the single MoSi$_2$ layer. According to the element line scanning result of the cross section of the coating, three elements Si, Mo, and Ti are all distributed in a diffusion gradient. The growth of (Ti, Mo)Si$_2$/MoSi$_2$ composite coating is dominated by the inward diffusion of Ti and Si. Ti is only concentrated in the outer layer of coating; Si is distributed in the whole coating and becomes less near the substrate; Mo exists steadily in the coating and is concentrated in the substrate. The above results show that when Si: Ti=20: 20 in the pack mixtures, the Ti-modified (Ti, Mo)Si$_2$ coating can be formed on the surface of MoSi$_2$ coating, but the (Ti, Mo)Si$_2$ layer is not continuous. As the Ti content in pack mixtures is further reduced, the intensity of diffraction peaks of (Ti, Mo)Si$_2$ phase is significantly weakened. So the co-deposition method cannot achieve the Ti deposition effectively.

Fig. 2 presents the coating phase component, BSE image of the cross section of coating, and EDS element line scanning result of the intermediate product coating after titanizing at 1000 °C for 5 h. Fig. 2a shows the intermediate coating consists of AlMoTi$_2$ and AlMo$_3$Ti$_x$ phases. Fig. 2b shows the BSE image and elemental line scanning result of the intermediate coating after titanizing. It can be seen that the Ti-modified layer is uneven. The outer layer is AlMoTi$_2$ phase and the transition layer between the AlMoTi$_2$ phase and the substrate is AlMo$_3$Ti$_x$ phase. The EDS element line scanning result in the cross section presents that the distribution of Al and Ti in the coating is relatively stable. The content of Al and Ti gradually reduces while the Mo content increases near the substrate. The element distribution shows that the formation of alloy phase in the coating is caused by the diffusion of Al and Ti elements. Because the metal bond between the metal elements has no saturation state, a gradient distribution of elements in the coating appears.

Fig. 3 presents the coating phase component, BSE image of the cross section of coating, and EDS element line scanning result of coating prepared by two-step pack cementation, i.e., titanizing and siliconizing. Fig. 3a shows that the (Ti, Mo)Si$_2$ and MoSi$_2$ phases exist in the coating after siliconizing. In addition, the weak diffraction peaks of TiSi and Al$_3$Mo phases can also be observed. The existence of Al is due to the introduction of trace Al in the titanizing process, and consequently Al is dispersed in the (Ti, Mo)Si$_2$ layer. BSE image and EDS element line scanning result of the coating prepared by two-step pack cementation are shown in Fig. 3b. The coating structure and element line scanning result are

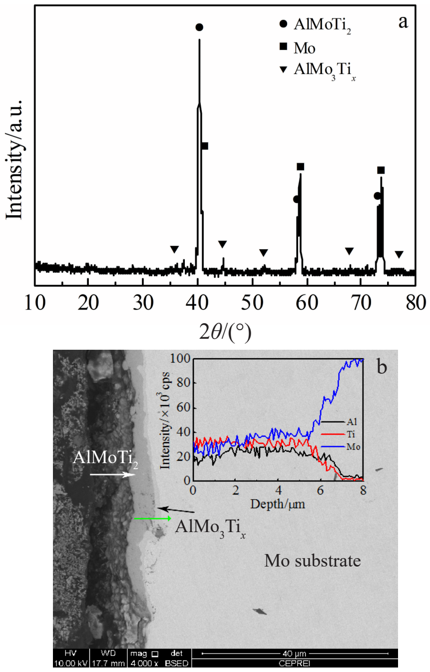

Fig.2 XRD pattern of coating after titanizing (a); BSE image and EDS element line scanning result of intermediate 40Ti-10NH$_4$F-50Al$_2$O$_3$ coating (b)

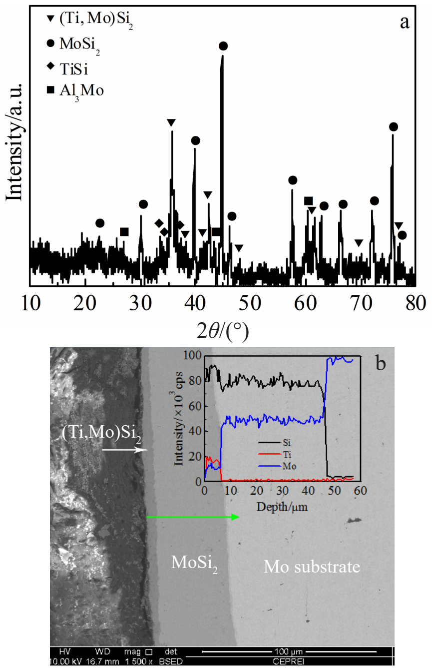

Fig.3 XRD pattern of coating prepared by two-step pack cementation method (a); BSE image and EDS element line scanning result of 40Si-10NH$_4$F-50Al$_2$O$_3$ coating (b)

similar to those of the coating prepared by co-deposition method. The outer layer consists of continuous (Ti, Mo)Si$_2$ phase with the thickness of 7~10 μm, and the second layer is the single MoSi$_2$ layer. The above results show that the Ti-modified MoSi$_2$ coating can be effectively prepared by the two-step pack cementation method.

2.2 Effect of siliconizing parameters on (Ti, Mo)Si$_2$/MoSi$_2$ composite coating prepared by two-step deposition method

After titanizing at 1000 °C, the specimens were treated through siliconizing process at 900~1100 °C. BSE images of cross-section of coating and element line scanning results are shown in Fig. 4. It can be seen that with increasing the siliconizing temperature, the coating structure does not change significantly. The coatings contain three layers: the outer layer is (Ti, Mo)Si$_2$ ternary compound; the second layer is MoSi$_2$; the layer between the MoSi$_2$ and Mo substrate is the Mo$_5$Si$_3$ transition layer. Furthermore, with increasing the siliconizing temperature, the thickness of (Ti, Mo)Si$_2$ ternary compound layer does not increase obviously. When the siliconizing temperature reaches 1100 °C, the thickness of MoSi$_2$ and Mo$_5$Si$_3$ transition layer increases significantly. Moreover, a certain amount of Al$_3$Mo precipitate can be observed in the (Ti, Mo)Si$_2$ layer near the interface of MoSi$_2$ layer. The siliconizing temperature exerts negligible effect on the coating structure. The growth rate of titanium-modified MoSi$_2$ coating is slightly lower than that of single MoSi$_2$ coating.

EDS analysis was conducted to determine the (Ti$_x$, Mo$_{1-x}$)Si$_2$ layer after siliconizing at 900~1100 °C, and the results are shown in Table 2. The (Ti$_x$, Mo$_{1-x}$)Si$_2$ ternary compound layer can be identified as (Ti$_{0.71}$, Mo$_{0.29}$)Si$_2$, (Ti$_{0.64}$, Mo$_{0.36}$)Si$_2$, and (Ti$_{0.28}$, Mo$_{0.72}$)Si$_2$ in the coatings after siliconizing at 900, 1000, and 1100 °C, respectively. The Ti content in (Ti$_x$, Mo$_{1-x}$)Si$_2$ phase ranges from 26at% to 75at%, which fits the (Ti$_x$, Mo$_{1-x}$)Si$_2$ phase with C40 structure[13]. Moreover, with increasing the siliconizing temperature, the proportion of Ti in (Ti, Mo)Si$_2$ is decreased and the proportion of Mo is increased, suggesting that Ti is gradually homogenized in the ternary alloy layer.

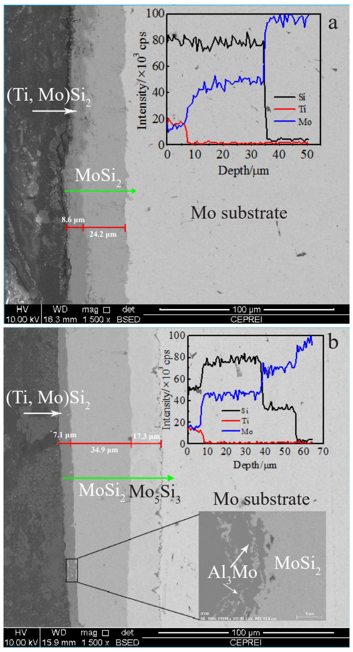

Fig.4 BSE images and EDS element line scanning results of coatings after siliconizing at 900 °C (a) and 1100 °C (b)

The effect of siliconizing time on the growth of modified silicide coating is shown in Fig. 5. It can be seen that the thickness of single MoSi$_2$ coating and (Ti, Mo)Si$_2$/MoSi$_2$ composite coating shows a nearly linear relationship with the square root of siliconizing time, which indicates that the growth of coatings conforms to the parabolic law $h=(K_pt)^{1/2}$ (h is the total thickness of the coating, t is the siliconizing time, K_p is the parabolic rate constant). According to the fitting equation in Fig. 5, the parabolic rate constant K_p of single MoSi$_2$ coating and (Ti, Mo)Si$_2$/MoSi$_2$ composite coating is 3.52×10^2 and 4.20×10^2 μm^2/h, respectively, suggesting that the growth rate of Ti-modified silicide coating is slightly lower than that of single siliconized coating. The above results show

Table 2 Results of EDS analysis for (Ti$_x$, Mo$_{1-x}$)Si$_2$ ternary compound layer

Siliconizing temperature/°C	Composition/at%			Phase component
	Si	Mo	Ti	
900	64.73	12.17	23.10	(Ti$_{0.71}$, Mo$_{0.29}$)Si$_2$
1000	64.88	14.22	20.9	(Ti$_{0.64}$, Mo$_{0.36}$)Si$_2$
1100	70.41	19.57	10.02	(Ti$_{0.28}$, Mo$_{0.72}$)Si$_2$

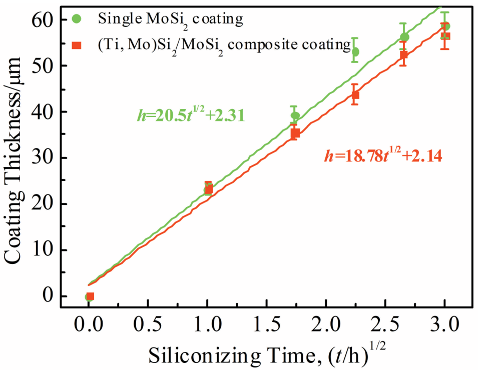

Fig.5 Relationship of coating thickness of single $MoSi_2$ coating and (Ti, Mo)Si_2/$MoSi_2$ composite coating with siliconizing time

that the outer (Ti, Mo)Si_2 layer has the diffusion blocking effect which can slow down the inner diffusion of Si.

2.3 Mechanism analysis of (Ti, Mo)Si_2/$MoSi_2$ composite coating formed by deposition of Ti and Si

Fig. 6 shows XRD patterns of coatings with different Si/Ti contents after co-deposition. The diffraction peaks of Si and Al_2O_3 can be observed. Meanwhile, the diffraction peaks of $TiSi_2$ also exist, which indicates that $TiSi_2$ is formed by the reaction of Si, Ti, and activator during co-deposition reaction. In addition, when the Si content in the pack mixtures is further increased, the intensity of diffraction peaks of Si is increased gradually, which means that part of unreacted Si remains in the pack mixtures. These results show that $TiSi_2$ is generated by the reaction of Si, Ti, and activator, leading to the insufficient Si and Ti sources (SiF_x and TiF_x) deposited on the surface of Mo substrate and the low deposition efficiency of coating prepared by the co-deposition method.

The chemical reactions in the co-deposition process are similar to those in the single siliconizing process, including the formation of volatile halide vapors of the master alloy elements, the deposition of gaseous halides in substrate surface, and the reactions of deposition elements with substrate[17,20,21]. In addition, the master elements possibly interact with each other. The main reactions occurring in the co-deposition process can be summarized as follows.

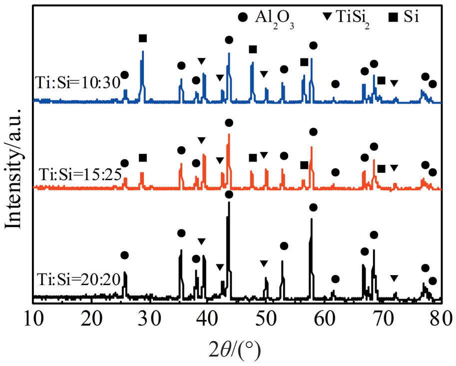

Fig.6 XRD patterns of coatings with different Si/Ti contents after co-deposition

(1) The decomposition of halide activator:

$$NH_4F\ (s) \rightarrow NH_3\ (g) + HF\ (g) \tag{1}$$

(2) The formation of volatile halide vapors of the master alloy elements:

$$Si\ (s) + xHF\ (g) \rightarrow SiF_x\ (g) + \frac{x}{2}H_2\ (g) \tag{2}$$

$$Ti\ (s) + xHF\ (g) \rightarrow TiF_x\ (g) + \frac{x}{2}H_2\ (g) \tag{3}$$

where x ranges from 1 to 4.

(3) The deposition of gaseous halides in substrate surface:

$$(x+1)SiF_x\ (g) \rightarrow Si\ (s) + xSiF_{x+1}\ (g) \tag{4}$$

$$(x+1)TiF_x\ (g) \rightarrow Ti\ (s) + xTiF_{x+1}\ (g) \tag{5}$$

$$TiF_x\ (g) + 2SiF_x\ (g) \rightarrow TiSi_2\ (s) + \frac{3x}{2}F_2\ (g) \tag{6}$$

$$2Si\ (s) + Ti\ (s) \rightarrow TiSi_2\ (s) \tag{7}$$

Since SiF_4 and TiF_4 are relatively stable, x ranges from 1 to 3.

(4) The reactions of deposition elements with substrate:

$$Si\ (s) + Ti\ (s) + Mo\ (s) \rightarrow (Ti, Mo)Si_2 \tag{8}$$

$$Si\ (s) + Mo\ (s) \rightarrow MoSi_2 \tag{9}$$

Fig. 7a shows the Gibbs free energy $\Delta_r G$-temperature T curves of the formation of gaseous halides of master alloy elements. It can be seen that the Gibbs free energies of the chemical reaction for generating SiF and TiF is all positive in

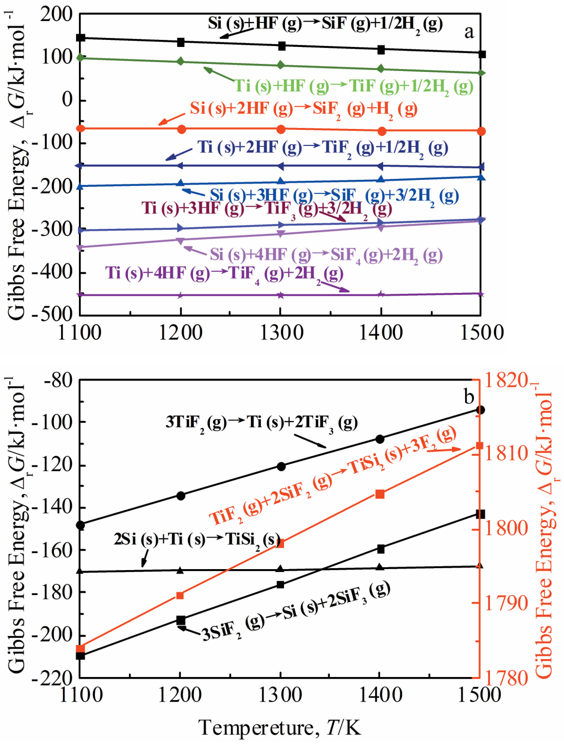

Fig.7 Gibbs free energy $\Delta_r G$-temperature T curves of formation of gaseous halides of master alloy elements (a) and gaseous halide deposition (b) during coating preparation process

the temperature range from 1100 K to 1500 K, indicating that the formation of SiF and TiF during the formation of gaseous halides is not supported in thermodynamics. In addition, the Gibbs free energy of formation of TiF_x (x=2~4) is lower than that of the formation of SiF_x (x=2~4) with the same x value, which indicates that the Ti-halides are more stable than Si-halides. In the reaction process, Ti is easier to react with activator than Si for forming gaseous halides.

The gaseous halides are diffused from the pack powder to the surface of Mo substrate and deposited at the interface between the gas phase and the matrix. Yang[19] and Majumdar[22] et al considered that the migration of difluoride controls the diffusion and deposition of gaseous halides to the substrate surface. The thermodynamic analysis results of possible reactions about the difluoride deposition and the interaction of Si and Ti are shown in Fig. 7b. It presents that the Gibbs free energies of the deposition reactions of SiF_2 and TiF_2 are all negative, i. e., the deposition of SiF_2 and TiF_2 is spontaneously. Meanwhile, the Gibbs free energy of the interaction between the gas phase SiF_2 and TiF_2 is positive, which indicates the reaction to form solid phase $TiSi_2$ by the gas phases is not supported in thermodynamics. The $TiSi_2$ can be formed by interaction between Si and Ti, because the Gibbs free energy of the interaction is negative at 1100~1500 K. However, due to the filler Al_2O_3, the reaction between silicon powder and titanium powder is inhibited. $TiSi_2$ is generated mainly through the gaseous halides containing Si and Ti deposited on the surface of Ti or Si powder, which explains the existence of a strong $TiSi_2$ diffraction peak and the fact that no diffraction peak of co-existence of silicon and titanium appears in the pack mixtures after packing process.

The XRD pattern of pack cementation components after titanizing process is shown in Fig. 8a. The filler Al_2O_3 and titanium-rich oxides can be observed. Fig. 8b shows the Gibbs free energy $\Delta_r G$-temperature T curves of possible reactions of TiF_2, Ti, and filler Al_2O_3. It can be seen that the reaction of TiF_2 and Al_2O_3 for formation of titanium-rich oxide (TiO) and free state AlF_3 is a spontaneous process. The inflection point appears at 1200~1300 K due to the transformation of TiO from β phase to α phase, according to the Ti-O phase diagram[23]. The Ellingham diagram shows that Al_2O_3 is more stable than TiO_2, and the reactions are spontaneous because F element shows more electronegativity than O element does, which makes F atom occupy the position of O atom and form AlF_3. The related chemical reaction is also verified in thermodynamics, as shown by the red line in Fig. 8b. In the low oxygen partial pressure environment, Ti combines with free O to form various titanium-rich oxides, as shown in Fig. 8a. In addition, the liquid phase AlF_3 contacts with Mo matrix in the form of free Al, which makes the free state Al and titanium-fluoride deposited on the Mo surface and diffused into the matrix to form a ternary alloy layer containing Al, Mo, and Ti.

In the process of siliconizing after titanizing, Si reacts with Ti-modified alloy layer to form (Ti, Mo)Si_2 layer, and then the Si element is diffused through the compound layer and interacts with the substrate forming the $MoSi_2$ layer. With the increase of siliconizing temperature, Si element is diffused along the substrate direction continuously and forms the Mo_5Si_3 transition layer between $MoSi_2$ and the substrate. The thickness of Mo_5Si_3 transition layer is increased gradually with increasing the siliconizing temperature. Ti element is only concentrated on the outer layer of coating due to the solid solution formed by Ti and Mo. When the titanium-fluoride is not deposited on the coating surface, the driving force of Ti diffusion to substrate is insufficient, and the asymmetric diffusion of Ti in the Mo substrate occurs[24,25], resulting in the fact that Ti element cannot be further diffused to the substrate. In the siliconizing process, a trace amount of Al introduced during the titanizing process can be diffused along the substrate direction. Since the diffusion rate of Al is faster than that of Si[10], the trace amount of Al_3Mo phase is precipitated in the (Ti, Mo)Si_2 layer near the interface of $MoSi_2$ layer.

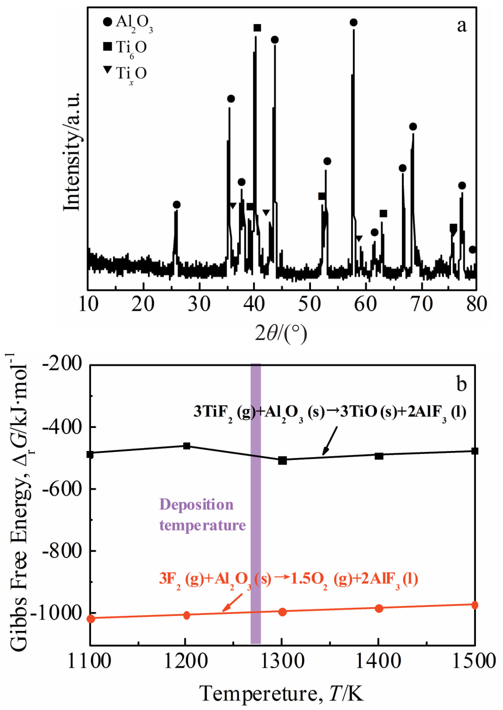

Fig.8 XRD pattern of pack cementation components after titanizing process (a); thermodynamic analysis of titanizing process (b)

2.4 Effects of Ti on oxidation resistance of coating

Cyclic oxidation tests of (Ti, Mo)Si_2/$MoSi_2$ composite coatings prepared by two-step method were conducted at 1200 °C. The oxidation performance of single $MoSi_2$ coating was also tested for comparison. The relationship between the mass gain per unit area of specimens and oxidation time is shown in Fig. 9. It can be seen that the oxidation process includes three stages of coating mass: linear increase, parabolic change, and increase with a decreased rise rate. At the initial stage of coating oxidation (<10 h), there is no dense oxide film on coating surface, and oxygen can react with the

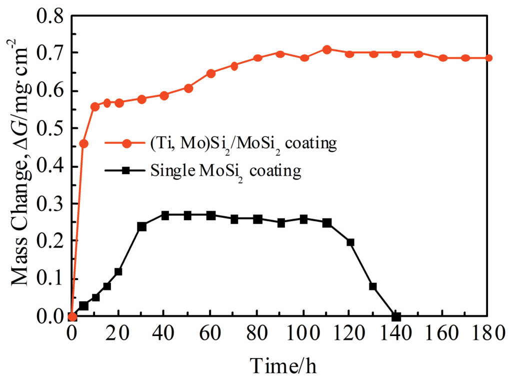

Fig.9 Mass change of single $MoSi_2$ coating and (Ti, Mo)Si_2/$MoSi_2$ composite coating after cyclic oxidation at 1200 °C in air

coating to form a dense oxide protective film. So the oxidation kinetics of the initial stage is a linear process[26,27]. As the oxide film covers the whole coating, a dense oxide layer is formed on the surface of the coating. After oxidation for 20 h, the oxidation rate in this stage is controlled by the internal diffusion of oxygen, so the relationship between the mass gain per unit area of the coating and oxidation time shows a parabolic change trend. For the single $MoSi_2$ coating, the rapid mass loss can be observed after exposure for 120 h, and the coating completely fails at 140 h. However, the (Ti, Mo)Si_2/$MoSi_2$ composite coating does not lose mass obviously after exposure for 180 h, which indicates that Ti element can effectively improve the oxidation resistance and prolong the oxidation resistance life of $MoSi_2$ coating.

Fig.10a and 10b show the BSE images of surface and cross-section of $MoSi_2$ coating after periodic oxidation at 1200 °C for 120 h. According to Fig10a, the MoO_3 phase exists in sheet form on the surface cracks of the coating. In Fig.10b, the coating consists of a complete $MoSi_2$ layer and a Mo_5Si_3 diffusion layer. A large number of Mo_5Si_3 phases formed by the decomposition of $MoSi_2$ into SiO_2 and Mo_5Si_3 during the oxidation process are distributed in the outer layer of the coating. During the periodic oxidation of the $MoSi_2$ coating at 1200 °C, the cracks in the coating are formed by thermal stress, which become the diffusion channels and make oxygen further react with the substrate. Although $MoSi_2$ layer is not completely transformed into Mo_5Si_3 layer, the hot cracks formed in the periodic oxidation process cannot be completely filled by SiO_2. When the cracks continue to expand due to thermal stress, the volatilization of MoO_3 is intensified, and then the protective coating fails. Fig. 10c and 10d show the BSE images of surface and cross-section morphologies of (Ti, Mo)Si_2/$MoSi_2$ compound coating after periodic oxidation at 1200 °C for 120 h. Fig. 10c shows that there is no MoO_3 phase volatilizing along the cracks on the coating surface, because the (Ti, Mo)Si_2 layer improves the high temperature stability of the coating and slows down the thermal stress impact rate to the coating in the periodic oxidation process. Fig. 10d presents a dense composite oxide layer consisting of SiO_2 and TiO_2 which is formed by the oxidation of (Ti, Mo)Si_2. This composite oxide layer can fill the surface cracks of the coating, thus inhibiting the pesting effect and significantly improving the oxidation resistance of the coating[28]. Moreover, during the oxidation process, the composite oxide layer can continuously block the oxygen

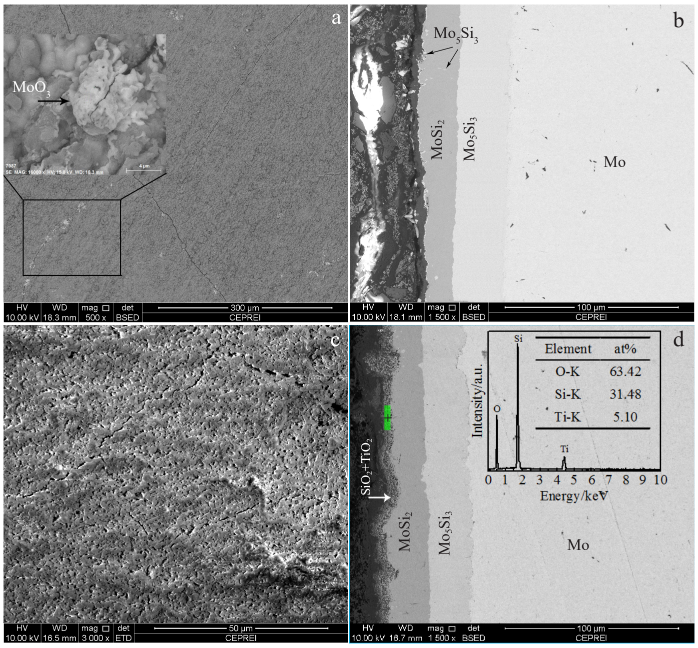

Fig.10 BSE images of surface (a, c) and cross-section (b, d) of $MoSi_2$ coating (a, b) and (Ti, Mo)Si_2/$MoSi_2$ composite coating (c, d) after cyclic oxidation at 1200 °C for 120 h

diffusion, prevent the coating from being the oxygen diffusion channel due to hot cracks, and avoid the direct contact reaction of oxygen with the substrate. Therefore, the Ti-modified silicide coating prepared by the two-step deposition method shows significantly better oxidation resistance in the periodic oxidation environment than the single silicide coating does.

3 Conclusions

1) The co-deposition process cannot achieve the titanium deposition effectively. The titanium-modified $MoSi_2$ coatings contain three layers: the outer layer is (Ti, Mo)Si_2 ternary compound; the second layer is $MoSi_2$; the layer between the $MoSi_2$ and the Mo substrate is the Mo_5Si_3 transition layer.

2) The siliconizing temperature exerts negligible effect on coating structure. The growth rate of titanium-modified $MoSi_2$ coating is slightly lower than that of the single $MoSi_2$ coating.

3) The growth of (Ti, Mo)Si_2/$MoSi_2$ composite coating is dominated by the inward diffusion of Ti and Si. Ti is only concentrated on the outer layer of coating. Si is diffused through the (Ti, Mo)Si_2 compound layer and interacts with the substrate to generate the $MoSi_2$ layer and Mo_5Si_3 transition layer. In the titanizing process, the free state AlF_3 can be introduced by the reaction among pack mixtures. In the subsequent siliconizing process, a trace amount of Al is precipitated in the form of Al_3Mo phases in the (Ti, Mo)Si_2 layer near the interface of $MoSi_2$ layer.

4) During the cyclic oxidation tests at 1200 °C, the (Ti, Mo)Si_2/$MoSi_2$ composite coatings do not lose mass obviously after exposure for 180 h. A dense composite oxide layer consisting of SiO_2 and TiO_2 can be formed by the oxidation of (Ti, Mo)Si_2. This composite oxide layer can fill the surface cracks of the coating and continuously block the oxygen diffusion, so the oxidation resistance of (Ti, Mo)Si_2/$MoSi_2$ composite coating in the periodic oxidation environment is far superior to that of the single silicide coating.

References

1 Zheng Xin, Bai Run, Wang Donghui *et al*. *Rare Metal Materials and Engineering*[J], 2011, 40(10): 1871 (in Chinese)

2 Osadnik M, Wrona A, Lis M *et al*. *Surface & Coatings Technology*[J], 2017, 318: 349

3 Chakraborty S P, Banerjee S, Sharma I G *et al*. *Journal of Nuclear Materials*[J], 2012, 403(1-3): 152

4 Lee E W, Cook J, Khan A *et al*. *JOM*[J], 1991, 43(3): 54

5 Opeka M M, Talmy I G, Zaykoski J A. *Journal of Materials Science*[J], 2004, 39(19): 5887

6 Zhu Y T, Stan M, Conzone S D *et al*. *Journal of the American Ceramic Society*[J], 1999, 82(10): 2785

7 Yanagihara K, Maruyama T, Nagata K. *Intermetallics*[J], 1995, 3(3): 243

8 Yanagihara K, Maruyama T, Nagata K. *Intermetallics*[J], 1996, 4(S1): 133

9 Tian Xiaodong, Guo Xiping, Sun Zhiping *et al*. *International Journal of Refractory Metals & Hard Materials*[J], 2014, 45: 8

10 Majumdar S. *Surface & Coatings Technology*[J], 2012, 206(15): 3393

11 Boettinger W J, Perepezko J H, Frankwicz P S. *Materials Science & Engineering A*[J], 1992, 155(1-2): 33

12 Heron A J, Schaffer G B. *Materials Science & Engineering A*[J], 2003, 352(1-2): 105

13 Li Wei, Fan Jinglian, Fan Yan *et al*. *Journal of Alloys and Compounds*[J], 2018, 740: 711

14 Tatemoto K, Ono Y, Suzuki R O. *Journal of Physics & Chemistry of Solids*[J], 2005, 66(2-4): 526

15 Yoon J K, Lee J K, Byun J Y *et al*. *Surface & Coatings Technology*[J], 2002, 160(1): 29

16 Erfanmanesh M, Reza B S, Khajelakzay M *et al*. *Ceramics International*[J], 2014, 40(3): 4529

17 Chakraborty S P. *Materials Today: Proceedings*[J], 2016, 3(9): 3071

18 Mevrel R, Duret C, Pichoir R. *Materials Science & Technology* [J], 1986, 2(3): 201

19 Yang Y, Chang Y A, Tan L *et al*. *Materials Science & Engineering A*[J], 2003, 361(1-2): 281

20 Majumdar S, Sharma I G, Suri A K. *International Journal of Refractory Metals & Hard Materials*[J], 2008, 26(6): 549

21 Yoon J K, Lee K H, Kim G H *et al*. *Journal of the Electrochemical Society*[J], 2004, 151(6): 309

22 Majumdar S, Sharma I, Samajdar I *et al*. *Journal of the Electrochemical Society*[J], 2008, 155(12): 734

23 Li Meishuan. *High Temperature Corrosion of Metals*[M]. Beijing: Metallurgical Industry Press, 2001: 21 (in Chinese)

24 Laik A, Kale G B, Bhanumurthy K. *Metallurgical & Materials Transactions A*[J], 2006, 37(10): 2919

25 Luo Mengzi, Liang Li, Lang Lin *et al*. *Computational Materials Science*[J], 2018, 141: 293

26 Cai Zhenyang, Liu Sainan, Xiao Lairong *et al*. *Surface & Coatings Technology*[J], 2017, 324: 182

27 Sharif A A. *Journal of Materials Science*[J], 2010, 45(4): 865

28 Azim M A, Gorr B, Christ H J *et al*. *Intermetallics*[J], 2017, 90: 103

钼表面包埋渗法制备(Ti, Mo)Si$_2$/MoSi$_2$涂层及其在1200 ℃周期性氧化环境下的氧化行为

何浩然[1,3]，刘 奇[1,2,3]，薄新维[1,2]，王小宇[1]，王焱辉[1]，姚志远[1]，韩校宇[1]，刘成超[1]

(1. 重庆材料研究院有限公司，重庆 400707)

(2. 国家仪表功能材料工程技术研究中心，重庆 400707)

(3. 重庆理工大学 化学化工学院，重庆 400054)

摘 要：利用连续沉积的包埋渗法，在钼表面制备了(Ti，Mo)Si$_2$/MoSi$_2$复合涂层。利用X射线衍射、扫描电子显微镜、能谱仪和热力学计算对涂层进行了表征与反应机理分析。结果表明，共沉积法无法实现Ti的有效沉积。先渗Ti、再渗Si的两步沉积工艺能有效制备Ti改性硅化物涂层。涂层分为3层，最外层为(Ti，Mo)Si$_2$三元化合物层，次外层为MoSi$_2$层，次外层与基体间为Mo$_5$Si$_3$过渡层。渗硅温度对涂层结构无明显影响。Ti改性硅化物涂层的生长速率略低于单一渗硅涂层的生长速率。(Ti，Mo)Si$_2$/MoSi$_2$复合涂层的形成由Ti、Si内扩散控制。Ti元素集中在涂层表层，Si元素通过(Ti，Mo)Si$_2$化合物层与基体作用形成MoSi$_2$层和Mo$_5$Si$_3$过渡层。渗Ti过程中，埋渗料间反应会引入游离态铝氟化物AlF$_3$。在随后的渗硅过程中，游离态Al以Al$_3$Mo的形式在(Ti，Mo)Si$_2$层中靠近MoSi$_2$层的上界面处析出。在1200 ℃周期性氧化过程中，(Ti，Mo)Si$_2$/MoSi$_2$复合涂层持续循环氧化180 h后未出现明显失重。(Ti，Mo)Si$_2$层氧化形成的SiO$_2$与TiO$_2$致密复合氧化层能填充涂层表面裂纹，持续阻碍氧扩散，因此其在周期性氧化环境下的抗氧化性能显著优于单一渗硅涂层。

关键词：包埋渗；钼硅化物；钛改性；抗氧化

作者简介：何浩然，男，1992年生，硕士，工程师，重庆材料研究院有限公司，重庆 400707，电话：023-60315487，E-mail：hehaoran@cmri.cc